

# Gate-structure optimization for high frequency power AlGaIn/GaN HEMTs\*

Wang Dongfang(王东方)<sup>1,2,†</sup>, Yuan Tingting(袁婷婷)<sup>1,2</sup>, Wei Ke(魏珂)<sup>1</sup>, Chen Xiaojuan(陈晓娟)<sup>1</sup>, and Liu Xinyu(刘新宇)<sup>1</sup>

(1 Institute of Microelectronics, Chinese Academy of Sciences, Beijing 100029, China)

(2 Graduated University of the Chinese Academy of Sciences, Beijing 100049, China)

**Abstract:** The influence of gate-head and gate-source-spacing on the performance of AlGaIn/GaN HEMTs was studied. Suggestions are then made to improve the performance of high frequency power AlGaIn/GaN HEMTs by optimizing the gate-structure. Reducing the field-plate length can effectively enhance gain, current gain cutoff frequency and maximum frequency of oscillation. By reducing the field-plate length, devices with  $0.35\ \mu\text{m}$  gate length have exhibited a current gain cutoff frequency of 30 GHz and a maximum frequency of oscillation of 80 GHz. The maximum frequency of oscillation can be further optimized either by increasing the gate-metal thickness, or by using a  $\tau$ -shape gate (the gate where the gate-head tends to the source side). Reducing the gate-source spacing can enhance the maximum drain-current and breakdown voltage, which is beneficial in enhancing the maximum output power of AlGaIn/GaN HEMTs.

**Key words:** AlGaIn/GaN HEMT; high frequency; gate structure; power

**DOI:** 10.1088/1674-4926/31/5/054003

**EEACC:** 2520D

## 1. Introduction

GaN-based materials exhibit high current density, high saturation velocity and high breakdown field. For this reason, AlGaIn/GaN high-electron-mobility transistors (HEMTs) are being developed for high power and high frequency applications. In recent years, there has been great progress in high frequency power AlGaIn/GaN HEMTs abroad. Ka-band, even W-band operations have been reported<sup>[1–3]</sup>. The output power at 40 GHz has reached  $10.5\ \text{W}/\text{mm}$ <sup>[1]</sup>.

In theory, reducing gate length can enhance  $f_T$  (current gain cutoff frequency) and  $f_{\text{max}}$  (maximum frequency of oscillation). Yet the gate length of X-band AlGaIn/GaN HEMTs has reached  $0.3\text{--}0.4\ \mu\text{m}$ , even  $0.25\ \mu\text{m}$ <sup>[4]</sup>. Gate lengths below  $0.25\ \mu\text{m}$  are still challenging for the domestic process, and deep sub-micron gates may cause serious short-channel effects such as threshold-voltage shift and soft pinch-off, high sub-threshold current and increased output conductance<sup>[5]</sup>.

On the other hand, T-shape gates (include  $\Gamma$ -shape gates) are widely used for sub-micron gates. Such gate-structure can lower the gate-resistance because of its increased cross-section, and a gate-head on the drain side serving as a field-plate can increase the breakdown voltage. Yet the introduction of a gate-head also increases the parasitical gate-capacitances ( $C_{\text{gs}}$  and  $C_{\text{gd}}$ ). It is known that low gate-resistance and low gate-capacitances are important for high frequency applications. So T-shape gates have a complicated influence on the performance of AlGaIn/GaN HEMTs. In this paper, we compare the DC and RF performance of AlGaIn/GaN HEMTs with different gate-structure parameters. The studied gate-structure parameters include gate-source spacing, gate-head length and gate-head location. It is indicated that the gate-head has a great influence on the frequency characteristics. By comparison, we drew some

conclusions on optimization of the gate-structure for high frequency power AlGaIn/GaN HEMTs.

## 2. Device structure and fabrication

The epitaxial wafer was provided by the Institute of Semiconductors of the Chinese Academy of Sciences.  $\text{Al}_{0.25}\text{Ga}_{0.75}\text{N}/\text{AlN}/\text{GaN}$  multilayers were grown on a sapphire substrate by MOCVD and the sheet resistance was  $370\ \Omega/\square$ . Ti/Al/Ni/Au for ohmic contact was deposited by evaporation, followed by rapid thermal annealing at  $870\ ^\circ\text{C}$  for 50 s. The ohmic contact resistivity was  $8.7 \times 10^{-6}\ \Omega \cdot \text{cm}^2$  measured by the four-probe method. Surface passivation was done using SiN (120 nm) film deposited by PECVD. A Ni/Au (40 nm/300 nm) gate with integrated gate-head was formed by the combined process of electron-beam lithography, dry-etch and evaporation. The actual gate length was measured to be  $0.35\ \mu\text{m}$  and the devices have a source-drain spacing of  $4\ \mu\text{m}$  and a gate-width of  $75\ \mu\text{m}$ . Figure 1 illustrates the devices' cross-section.

For convenience of comparison, the fabricated devices

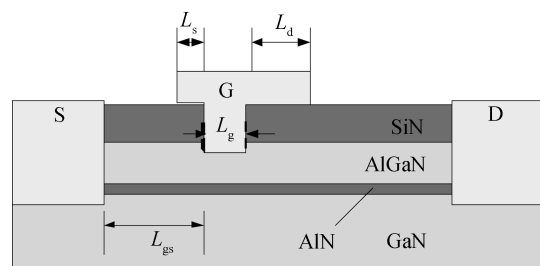


Fig. 1. Cross-section of the devices.

\* Project supported by the National Natural Science Foundation of China (No. 60890191).

† Corresponding author. Email: wdf0155@sina.com

Received 20 October 2009, revised manuscript received 12 February 2010

© 2010 Chinese Institute of Electronics

Table 1. Five compared groups.

Group	$L_d$ ( $\mu\text{m}$ )	$L_s$ ( $\mu\text{m}$ )	$L_{gs}$ ( $\mu\text{m}$ )
No. 1	0.2–1	0.2	1
No. 2	0.2	0.2–0.7	1
No. 3	0.2	0.7	1
	0.45	0.45	1
	0.7	0.2	1
No. 4	0.2	0.2	0.7–1.5
No. 5	0.2 or 0.7	0.2	2.3

were divided into five groups shown in Table 1. In the five groups, gate-head on the drain side ( $L_d$ ), gate-head on the source side ( $L_s$ ), gate-head location, and gate-source spacing ( $L_{gs}$ ) are changed respectively. (The No. 5 group was specially added for breakdown-voltage comparison, because their breakdown voltage is degraded to the measurement range of our apparatus.) For each group, only one parameter was variable and each kind of device had members of no less than 5.

### 3. DC characteristics

It is known that the maximum RF output power of a transistor operating at A-class can be estimated by  $P_{out,max} = \frac{V_{br}I_{DSS}}{8}$ , where  $V_{br}$  is the breakdown voltage,  $I_{DSS}$  is the maximum drain current. So increasing  $I_{DSS}$  and  $V_{br}$  is critical for power transistors.

Measurements for the five groups indicated that  $I_{DSS}$  and transconductance ( $g_m$ ) increase when  $L_{gs}$  was reduced. Yet such DC characteristics do not obviously alter, if  $L_d$ ,  $L_s$ , or the gate-head location is changed. Figure 2 shows the  $I_{DS}-V_{DS}$  characteristic for two kinds of HEMTs with different  $L_{gs}$  and Figure 3 shows their transconductance ( $g_m$ ) and  $I_{DS}-V_g$  characteristics. The HEMTs with  $L_{gs} = 0.7 \mu\text{m}$  exhibit  $I_{DSS}$  of 719 mA/mm and maximum  $g_m$  of 301 mS/mm. Yet the ones with  $L_{gs} = 1.5 \mu\text{m}$  exhibit  $I_{DSS}$  of 655 mA/mm and  $g_m$  of 273 mS/mm.

Some studies have proved that large gate field-plate ( $L_d$ ) and large gate-drain spacing ( $L_{gd}$ ) can increase the breakdown voltage ( $V_{br}$ )<sup>[6,7]</sup>. In this work, most devices exhibited  $V_{br}$  of 100 V or over, which exceeded the measurement range of our apparatus. Only the devices of group No.5, which have  $L_{gd}$  of 1.4  $\mu\text{m}$  (i.e.  $L_{gs} = 2.3 \mu\text{m}$ ), exhibited a breakdown voltage lower than 100 V. Among these devices, the ones with  $L_d = 0.2 \mu\text{m}$  exhibited a breakdown voltage of 62 V, and the others with  $L_d = 0.7 \mu\text{m}$  exhibited a breakdown voltage of 74 V.

### 4. Frequency characteristics

Experiments also indicated that the frequency characteristics of AlGaIn/GaN HEMTs are greatly influenced by gate-head lengths and gate-head location. Yet reducing the gate-source spacing does not enhance  $f_T$  and  $f_{max}$  as expected. This is because reducing  $L_{gs}$  also increases the gate capacitance which balances the increased  $g_m$ <sup>[8]</sup>.

The gate with a gate-head tending to the drain side is called a  $\Gamma$ -shape gate. Such gates are widely used in power AlGaIn/GaN HEMTs because the gate-head can serve as a field-plate which can increase the breakdown voltage. Fig. 4 shows the RF-gains for devices with different field-plate lengths (group No. 1). It can be seen that  $h_{21}$  (current gain) and

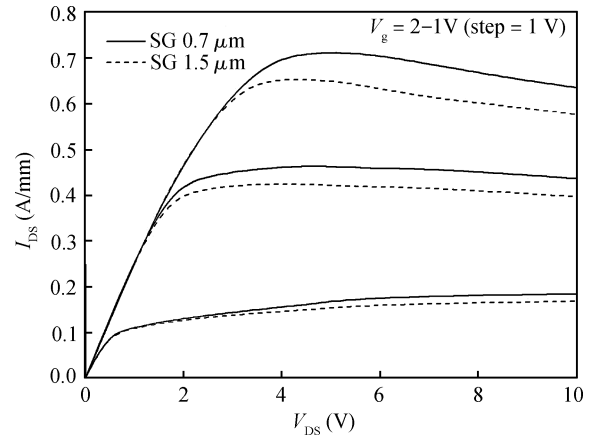


Fig. 2.  $I_{DS}-V_{DS}$  characteristic for devices with  $L_{gs} = 0.7 \mu\text{m}$  and  $L_{gs} = 1.5 \mu\text{m}$  respectively.

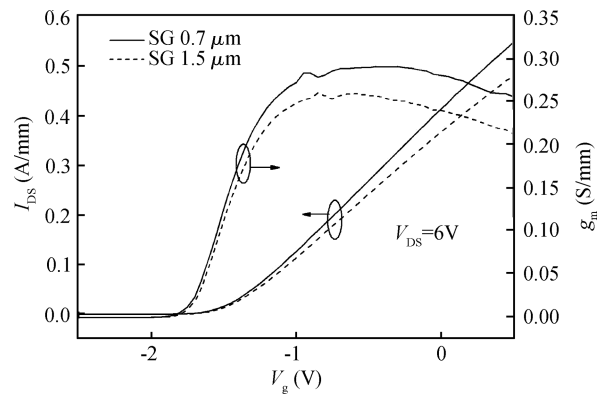


Fig. 3. Transconductance ( $g_m$ ) and  $I_{DS}-V_g$  characteristics for devices with  $L_{gs} = 0.7 \mu\text{m}$  and  $L_{gs} = 1.5 \mu\text{m}$  respectively.

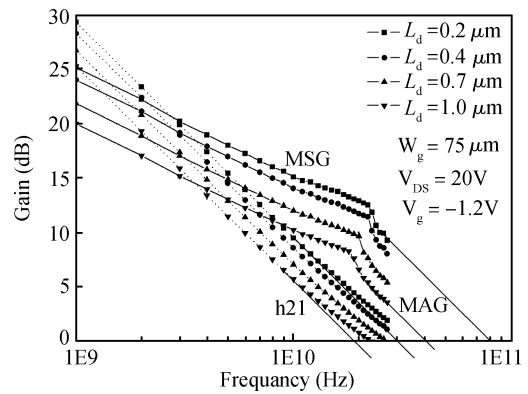


Fig. 4. Small-signal RF-gains of devices with different field-plate lengths.

MSG/MAG (maximum stable gain/maximum available gain) increase with reduced field-plate length. At 8 GHz, the device with  $L_d = 1.0 \mu\text{m}$  has MSG of 11.1 dB. If the length is reduced to  $0.2 \mu\text{m}$ , the MSG reaches 16.0 dB. Moreover, the turning frequency from MAG to MSG also increases. This redounds to enhance gain at high frequency. At 30 GHz, the MAG is about 2.7 dB for the former, and is 8.5 dB for the latter. Figure 5 shows  $f_T$ ,  $f_{max}$  and MAG for devices with different field-plate lengths.

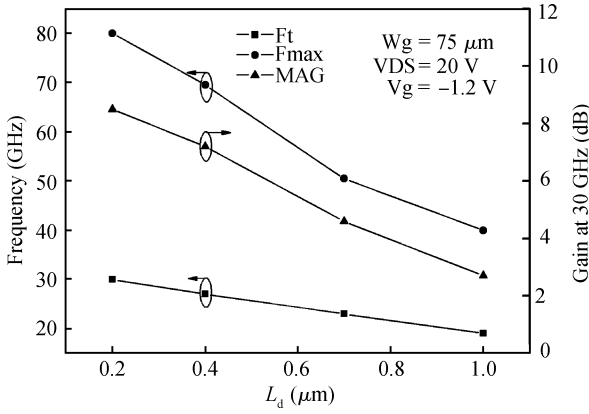


Fig. 5.  $f_T$ ,  $f_{max}$  and MAG of devices with different field-plate lengths.

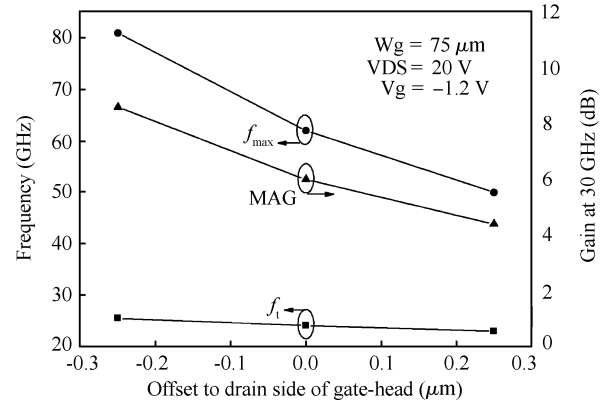


Fig. 7.  $f_T$ ,  $f_{max}$  and MAG for devices with different gate-head locations (or gate shapes).

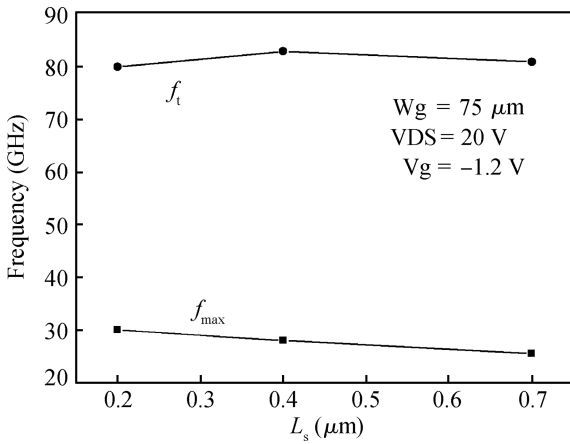


Fig. 6.  $f_T$ ,  $f_{max}$  of devices with different  $L_s$ .

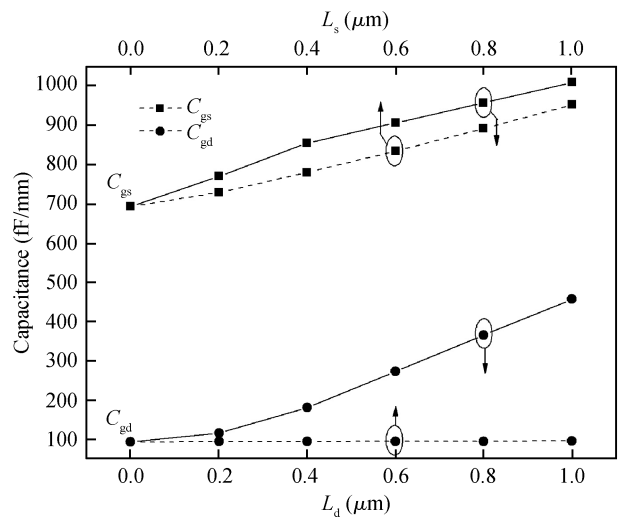


Fig. 8. Simulated relations of gate capacitances versus  $L_d$  and  $L_s$  respectively.

In this paper, we call the gate where the gate-head tends to the source side a  $\tau$ -shape gate. Figure 6 shows the  $f_T$ ,  $f_{max}$  of HEMTs with different  $L_s$  (group No. 2). Compared with Fig. 5, it can be seen that  $L_s$  has less influence on the frequency than  $L_d$ . With  $L_s$  reduced,  $f_T$  increases. But  $f_{max}$  does not vary much, and a peak value even occurs at  $L_s = 0.4 \mu\text{m}$ . This indicates that the gate-resistance and gate-capacitance are optimized for  $f_{max}$  at this point. The devices with  $L_s = 0.2 \mu\text{m}$  have smaller parasitical gate-capacitances and higher  $f_T$  than the ones with  $L_s = 0.4 \mu\text{m}$ , yet their  $f_{max}$  is lower. The only explanation is that the former has too high a gate-resistance which results from the reduction of the gate cross-section. Both reducing  $L_d$  and reducing  $L_s$  will cause cross-section reduction. So increasing the gate-metal thickness is necessary, if gate-head length is reduced by much.

Either the  $\Gamma$ -shape gate or  $\tau$ -shape gate can be considered as a special T-shape gate. The only difference is their gate-head location. Figure 7 shows  $f_T$ ,  $f_{max}$  and MAG of devices with different gate-head locations. The horizontal axis is the offset to drain side of the gate-head, compared with the normal T-shape gate. It can be seen that moving the gate-head from the drain side to the source side can enhance  $f_T$ ,  $f_{max}$  and MAG. The three kinds of gates have equal gate-resistance, yet the  $\tau$ -shape gate exhibits better frequency characteristics.

$L_d$  and  $L_s$  can cause parasitical gate-capacitances. We have used a finite-element two-dimensional simulator (Silvaco At-

las) to investigate the gate capacitances for devices illustrated in Fig. 1. In one simulation,  $L_s$  was set to 0, and  $L_d$  varied from 0 to 1  $\mu\text{m}$ . In another simulation,  $L_d$  was set to 0, and  $L_s$  varied from 0 to 1  $\mu\text{m}$ . Figure 8 shows the relations of gate capacitances versus  $L_d$  and  $L_s$  respectively. With  $L_s$  increasing,  $C_{gs}$  increases and  $C_{gd}$  nearly keep constant. Yet with  $L_d$  increasing, both  $C_{gs}$  and  $C_{gd}$  increase. We believe this is due to the field-plate function of the  $L_d$  part. When  $L_d$  increases, the electric field beneath the gate-foot decreases, so the depletion-mode region reduced, which makes  $C_{gs}$  also increase. The simulations indicate that  $L_d$  has greater effect on both  $C_{gs}$  and  $C_{gd}$  than  $L_s$ . This can explain why reducing  $L_d$  can improve frequency characteristics more effectively than reducing  $L_s$ .

### 5. Gate-structure optimization

So far the implementation of gate lengths below 0.25  $\mu\text{m}$  is still challenging for the domestic process of AlGaIn/GaN HEMTs. Moreover, such deep sub-micron gates may cause serious short channel effects<sup>[5]</sup>. So it is significant to improve the frequency characteristics by optimizing the gate-structure.

From the above experiments, we can make suggestions to improve the frequency characteristics of AlGaIn/GaN HEMTs.

By reducing the gate-field-plate length, the gain,  $f_T$  and  $f_{max}$  can be effectively enhanced. Yet reducing the gate-field-plate reduced the gate cross-section. The gate-resistance will increase, which can limit the enhancement of  $f_{max}$ . So if the gate-field-plate is reduced by much, it is preferable to increase the gate-metal thickness.

$L_s$  has less influence on the frequency characteristics than  $L_d$ . Increasing  $L_s$  can reduce the gate resistance. So  $f_{max}$  can also be optimized by using a  $\tau$ -shape gate, except to increase the gate-metal thickness.

Either reducing the gate field-plate or using a  $\tau$ -shape-gate improves the frequency characteristics at the expense of degrading the breakdown voltage (the  $\tau$ -shape gate also has a small gate field-plate). Increasing the gate-drain spacing can enhance the breakdown voltage of AlGaIn/GaN HEMTs. When the source-drain spacing is fixed, it is preferable to locate the gate as near the source side as possible (i.e. reducing the gate-source spacing). Moreover, reducing the gate-source spacing can also enhance the maximum drain current. So reducing the gate-source spacing is beneficial to enhancement of the maximum output power of AlGaIn/GaN HEMTs.

## 6. Conclusion

We have studied the DC and RF performance of AlGaIn/GaN HEMTs with different gate-structures. From the results, we have made suggestions to improve the performance of high frequency power AlGaIn/GaN HEMTs by optimizing the gate-structure. Reducing the field-plate length can effectively enhance gain,  $f_T$  and  $f_{max}$ .  $f_{max}$  can be further optimized either by increasing the gate-metal thickness, or by using a  $\tau$ -

shape gate (a gate where the gate-head tends to the source side). These approaches for improving frequency characteristics are especially significant when difficulties exist with reducing the gate length. In order to enhance the maximum output power, it is preferable to reduce the gate-source spacing, which can enhance the maximum drain-current and breakdown voltage.

## References

- [1] Palacios T, Chakraborty A, Rajan S, et al. High-power AlGaIn/GaN HEMTs for Ka-band applications. *IEEE Electron Device Lett*, 2005, 26(11): 781
- [2] Inoue T, Ando Y, Miyamoto H, et al. 30-GHz-band over 5-W power performance of short-channel AlGaIn/GaN heterojunction FETs. *IEEE Trans Microw Theory Tech*, 2005, 53(1): 74
- [3] Micovic M, Kurdoghlian A, Hashimoto P, et al. GaN HFET for W-band power applications. *IEEE International Electron Devices Meeting*, 2006: 1
- [4] Jimenez J L, Chowdhury U. X-band GaN FET reliability. *IEEE 46th International Reliability Physics Symposium*, 2008: 429
- [5] Palacios T, Chakraborty A, Heikman S, et al. AlGaIn/GaN high electron mobility transistors with InGaIn back-barriers. *IEEE Electron Device Lett*, 2006, 27(1): 13
- [6] Karmalkar S, Mishra U K. Enhancement of breakdown voltage in AlGaIn/GaN high electron mobility transistors using a field plate. *IEEE Trans Electron Devices*, 2001, 48(8): 1515
- [7] Kikkawa T, Makiyama K, Imanishi K, et al. High  $f_{max}$  GaN-HEMT with high breakdown voltage for millimeter-wave applications. *IEEE Compound Semiconductor Integrated Circuit Symposium*, 2007: 1
- [8] Russo S, Carlo A D. Influence of the source-gate distance on the AlGaIn/GaN HEMT performance. *IEEE Trans Electron Devices*, 2007, 54(5): 1071